The spatial dynamics of vertical migration by *Microcystis aeruginosa* in a eutrophic shallow lake: A case study using high spatial resolution time-series airborne remote sensing

P. D. Hunter,[1] *A. N. Tyler, N. J. Willby, and D. J. Gilvear*
School of Biological and Environmental Science, University of Stirling, Stirling, FK9 4LA, Scotland, United Kingdom

Abstract

Time-series airborne remote sensing was used to monitor diurnal changes in the spatial distribution of a bloom of the potentially toxic cyanobacterium *Microcystis aeruginosa* in the shallow eutrophic waters of Barton Broad, United Kingdom. High spatial resolution images from the Compact Airborne Spectrographic Imager (CASI-2) were acquired over Barton Broad on 29 August 2005 at 09:30 h, 12:00 h, and 16:00 h Greenwich mean time. Semiempirical water-leaving radiance algorithms were derived for the quantification of chlorophyll *a* ($R^2 = 0.96$) and C-phycocyanin ($R^2 = 0.95$) and applied to the CASI-2 imagery to generate dynamic, spatially resolving maps of the *M. aeruginosa* bloom. The development of the bloom may have been fostered by a combination of the recent improvements in the ambient light environment of Barton Broad, allied to the acute depletion of bioavailable nutrient pools, and stable hydrodynamic conditions. The vertical distribution of *M. aeruginosa* was highly transient; buoyant colonies formed early morning and late afternoon near-surface aggregations across the lake during periods of nonturbulent mixing (wind speed <4 m s^{-1}). However, the extent of these near-surface aggregations was highly spatially variable, and nearshore morphometry appeared to be crucial in creating localized regions of nonturbulent water in which pronounced and persistent near-surface aggregations were observed. The formation of these near-surface scums would have been vital in alleviating light starvation in the turbid waters of Barton Broad. The calm water refuges in which persistent near-surface accumulations occurred may have been an important factor in determining the persistence of the bloom.

Cyanobacteria (blue-green algae) are an important component of the microbial biodiversity of aquatic ecosystems and fulfill key roles within biogeochemical cycles. However, in nutrient-enriched waters, prolific cyanobacterial growth can lead to the development of mass populations, as either nuisance blooms, scums, or biofilms. Mass populations of cyanobacteria can have severe ecological repercussions for aquatic ecosystems. Moreover, as many of the bloom-, scum-, and biofilm-forming genera produce a range of potent toxins, mass populations of cyanobacteria can often pose significant risks to animal and human health (Codd et al. 1999, 2005). This is a particular concern in lakes because they are often highly used for recreational purposes.

Incidences of cyanobacterial blooms in lakes have increased significantly over recent years as a result of eutrophication (Paerl 1988). However, the development of cyanobacterial blooms in eutrophic lakes is often dependent on factors other than just nutrient enrichment, and often blooms may be a response to several mitigating factors (Scheffer et al. 1997; Hyenstrand et al. 1998; Dokulil and Teubner 2000). Indeed, the ability of some cyanobacteria to adjust their cell buoyancy and thereby regulate their vertical station within the water column has been proposed as one of the main mechanisms through which cyanobacteria are able to dominate the phytoplankton flora of turbid nutrient-enriched lakes (van Rijn and Shilo 1985; Reynolds et al. 1987).

Buoyancy regulation in gas-vacuolate cyanobacteria is achieved through two related mechanisms: synthesis and turgor-pressure–induced collapse of gas vesicles, and the adjustment of gas-vesicle buoyancy using cell ballast afforded by the photosynthetic production or metabolic utilization of carbohydrates (Oliver and Walsby 1984; Kromkamp et al. 1988; Oliver 1994). In lakes, the latter mechanism allows some species of cyanobacteria to undertake rapid vertical migrations to near-surface waters (e.g., *Anabaena*, *Microcystis*) (Reynolds et al. 1987; Humphries and Lyne 1998). Similar behavior can also be observed in several species of marine cyanobacteria (e.g., *Trichodesmium*) (Villareal and Carpenter 1990). The ability of cyanobacteria to perform such rapid migrations has great ecological significance: vertical migration essentially enables cyanobacteria to trawl for scattered resources during periods of stress (i.e., low light or nutrient limitation) (Takamura and Yasuno 1984). It is not merely coincidence that the most proficient buoyancy-regulating ecotypes (e.g., *Anabaena*, *Microcystis*) are amongst the most stress-tolerant (S-adapted) of freshwater phytoplankton species (Reynolds et al. 2002; Reynolds 2006).

Vertical migration by buoyancy-regulating cyanobacteria can have a profound effect upon both the vertical and the horizontal distribution of cyanobacteria in lakes. The transition between states of negative and positive cell buoyancy can occur over a matter of hours. Consequently, changes in the vertical distribution of buoyancy-regulating cyanobacteria can be very rapid indeed (Reynolds et al. 1987). Moreover, as the vertical station of cyanobacteria determines entrainment or disentrainment within surface and subsurface currents, vertical heterogeneity can often be compounded by the downwind accumulation of buoyant cyanobacterial cells entrained within advective currents (Hedger et al. 2002, 2004). Ultimately, this can lead to marked patchiness in spatial distribution of cyanobacteria in lakes.

In situ point-scale sampling is seldom able to adequately describe pronounced patchiness in the distribution of cyanobacteria. This can present a significant obstacle to the effective monitoring of cyanobacterial populations, and may complicate efforts to elucidate the nature of processes controlling their spatial and temporal distribution (Rantajärvi et al. 1998; Kutser 2004). Remote sensing platforms have the ability to provide spatially synoptic monitoring of waterbodies. Remote-sensing–based techniques for the quantification of chlorophyll *a* (Chl *a*) have proven effective for monitoring the distribution of phytoplankton blooms (Kutser et al. 2006; Reinart and Kutser 2006; Tyler et al. 2006). However, such an approach does not enable the abundance of cyanobacteria to be determined separately from other Chl *a*–containing eukaryotic algae. Consequently, there is currently much interest in the development of optical techniques for the detection of cyanobacteria blooms, not only in lakes, but also in other inland and coastal waters.

Cyanobacteria have unique optical properties that distinguish them from other species of eukaryotic algae (Hunter et al. 2008). The optical signatures of cyanobacteria are strongly influenced by the photosynthetic biomarker pigment C-phycocyanin (C-PC), which has a diagnostic absorption maximum at c. 615 nm. The presence and magnitude of the C-PC–related absorption feature in remote sensing spectra can therefore be used as an index of cyanobacterial abundance. Semiempirical algorithms for the quantification of C-PC have been developed that enable the estimation of cyanobacterial biomass from remotely sensed data (Dekker 1993; Schalles and Yacobi 2000; Hunter et al. 2008). In addition, Simis et al. (2005, 2007) have recently developed and validated a semianalytical algorithm for use with products from the European Space Agency's Medium Resolution Imaging Spectrometer (MERIS) aboard Envisat. To date, both semiempirical and semianalytical approaches have been shown to be effective for estimating the concentration of C-PC in lakes where the phytoplankton assemblage is largely dominated by phycocyanin-rich cyanobacteria (i.e., high C-PC and C-PC : Chl *a*) (Dekker 1993; Schalles and Yacobi 2000; Simis et al. 2005).

The ability to detect the presence of C-PC in waterbodies using satellite or airborne sensors requires a narrow spectral band positioned in proximity to the C-PC absorption maximum (i.e., centered at ~620 nm and 10–15 nm wide). MERIS has a suitable spectral band set configuration, signal-to-noise ratio, and swath-width coverage for the operational retrieval of C-PC concentrations in inland and coastal waters. However, although the spatial resolution of MERIS (c. 300 m) is conducive to the observation of large lakes and coastal waters, it is not suitable for the observation of smaller inland waters. Furthermore, the coarse spatial resolution of MERIS means it is not able to resolve fine-scale heterogeneity (<300 m) in the distribution of cyanobacteria. The prototype hyperspectral sensor Hyperion aboard the National Aeronautics and Space Administration's Earth Observing–1 satellite also has a suitable spectral coverage and resolution and, in comparison to MERIS, offers a higher spatial resolution (30 m). Even so, the spatial resolution of Hyperion may still not be sufficient to resolve fine-scale patchiness of cyanobacterial blooms in lakes and coastal waters (Kutser 2004).

In this context, the high spatial resolution data provided by airborne imaging spectrometers (c. <5 m) may prove valuable for expeditious research until comparable satellite products become available. Many imaging spectrometers have hyperspectral capabilities, or customizable spectral band set configurations, which makes them ideally suited to the resolution and retrieval of C-PC in waterbodies. Furthermore, in comparison to satellite-mounted sensors, airborne systems also offer increased flexibility in deployment so that high-resolution time-series data can be acquired of cyanobacterial bloom dynamics.

The ability to monitor cyanobacteria using remote sensing platforms affords an opportunity to further exploit such technologies for the purposes of lake monitoring. Moreover, there is an opportunity to use such data to examine the spatial and temporal dynamics of cyanobacteria blooms in lakes. Vertical migration by cyanobacteria has been studied extensively, but only at the laboratory or point scale and, as such, there would seem to be much to be gained by using remote sensing to examine this phenomenon at a truly synoptic lake scale. Thus, the aim of this study was to use time-series remote sensing surveillance, in conjunction with in situ monitoring data, to examine the spatial dynamics of vertical migration, and to examine how such behavior may foster cyanobacteria dominance in turbid shallow lakes.

Methods

Study site—The Norfolk Broads are a series of small and shallow temperate lakes in eastern England. These shallow lowland lakes range in size from 0.001 to 1.3 km² and many retain a hydrological connection through a network of rivers, canals, and drainage ditches. Barton Broad (52°44′N, 1°30′E) is the second largest of the Norfolk Broads with a surface area of c. 0.6 km² and a total water volume of c. 804 × 10³ m³ (Fig. 1). Barton Broad is very shallow (mean depth ~1.4 m), and has a relatively uniform flat-bottomed bathymetry. The lake endures a strong fluvial influence from the River Ant (the main inflow and outflow), which ensures that it is regularly flushed and
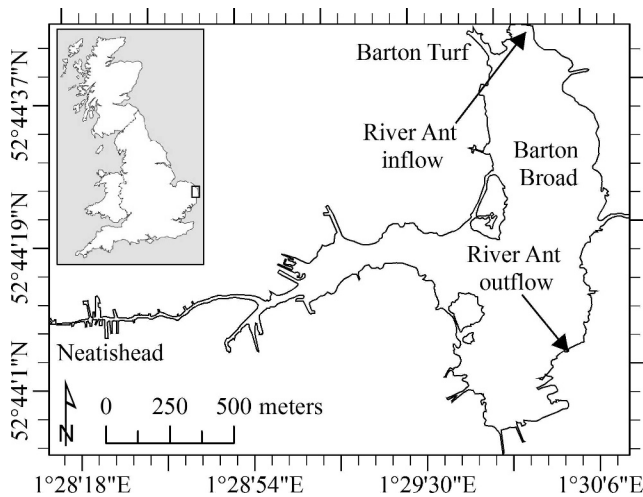
Fig. 1. Map of Barton Broad (52°44′N, 1°30′E), Norfolk, and its location within the United Kingdom (inset).

remains well-mixed throughout the year (Phillips et al. 2005). The mean residence time is approximately 16 d, although this varies between 10 d in winter months and 25 d in summer months (Phillips and Kerrison 1991).

The ecological status of Barton Broad declined from the 1950s onwards as a result of eutrophication, but has improved over recent years because of restoration efforts (Madgwick 1999; Phillips et al. 2005). The phytoplankton community of Barton Broad pre-restoration was dominated by centric diatoms (*Stephanodiscus* spp.) and filamentous (*Planktothrix agardhii* and *Limnothrix redekei*) and heterocystous N-fixing (*Anabaena* spp. and *Aphanizomenon flos-aquae*) cyanobacteria (Phillips et al. 2005). Since the implementation of the restoration measures, there has been a gradual change in floristic composition. The most notable response has been the replacement of centric diatoms by pennate species, and a marked decrease in the abundance of filamentous and N-fixing cyanobacteria. However, in the summers of 2005 and 2006, unprecedented blooms of the colonial, and potentially toxic, cyanobacterium *Microcystis aeruginosa* occurred on the lake.

Remote sensing data acquisition and analysis—Diurnal time-series imagery of Barton Broad was acquired on 29 August 2005 using the compact airborne spectrographic imager (CASI-2) in response to a cyanobacterial bloom largely comprised of *M. aeruginosa*. CASI-2 was operated by the United Kingdom's National Environment Research Council's Airborne Remote Sensing Facility (NERC ARSF) aboard a Dornier 228-101 aircraft. Three data acquisition sorties were flown over the lake at approximately 09:30 h, 12:00 h, and 16:00 h Greenwich mean time (GMT). Each data sortie involved the acquisition of four overlapping image flight lines to ensure that synoptic coverage of the lake was obtained.

CASI-2 was operated in spatial mode using the band set configuration detailed in Table 1; this included spectral bands centered at 620 and 670 nm to target the absorption features associated with C-PC and Chl *a* respectively. The NERC ARSF aircraft was deployed at a flight altitude of 1250 m to provide imagery with a spatial resolution of 2.5 m. The acquired image data were processed and analyzed in the RSI ENVI version 4.3 software environment. The image processing procedures included: (1) a correction for the effects of variable atmospheric path length; (2) a dark-pixel correction for atmospheric scattering effects (Hadjimitsis et al. 2004; Vincent et al. 2004; Tyler et al. 2006); and (3) image-to-image normalization using the empirical line method (to correct for inter-scene variations in illumination and solar zenith angles [$\theta = 43.2$–$57.1°$]).

The dark-pixel atmospheric correction method is somewhat limited by the fact that the resulting image can only be corrected to approximate the water-leaving radiance ($L_w[\lambda]$) (W m^{-2} nm^{-1} sr^{-1}) and not the preferential measurement of remote sensing reflectance ($R_{rs}[\lambda]$). The dark-pixel correction also cannot correct for the effects of atmospheric absorption. However, because the objective here was not to derive operational algorithms for Chl *a* and C-PC quantification, the use of a dark pixel atmospheric correction was considered sufficient.

Band ratios for the quantification of Chl *a* and C-PC applicable to the band set configuration of the CASI-2 sensor were identified from the literature. The band ratio

Table 1. The band set configuration of CASI-2 used for the acquisition of data over Barton Broad; the nearest equivalent channels of the Sea-viewing Wide Field-of-View Sensor (SeaWiFS) and Medium Resolution Imaging Spectrometer (MERIS) are also shown.

Band	Center (nm)	Width (nm)	Start (nm)	End (nm)	SeaWiFS	MERIS
1	412	20	402.81	422.15	1	1
2	443	20	432.72	453.87	2	2
3	490	20	480.37	499.84	3	3
4	510	20	501.61	519.33	4	4
5	555	20	545.97	565.53	5	5
6	620	20	610.10	629.76		6
7	670	20	660.19	679.92	6	7
8	682.5	5	681.72	685.31		8
9	710	10	705.07	715.86		9
10	752	15	744.76	759.10	7	10
11	762	5	760.90	764.51	7	11
12	775	20	766.31	784.37	7	12
13	820	10	815.13	824.18		

used for the quantification of Chl *a* was $[L_w(710) : L_w(670)]$ (Han and Rundquist 1997; Dall'Olmo et al. 2005), whereas the band ratio for the quantification of C-PC was $[L_w(710) : L_w(620)]$ (Simis et al. 2005, 2007). The band ratios were applied to the CASI-2 imagery and the values were extracted from the position of each sampling station on the lake. The resulting data sets were $\log_{10}$-transformed to improve linearity, and least-squares regression analysis was performed between the co-registered band ratio values and measured pigment concentrations to generate semiempirical algorithms for the estimation of Chl *a* and C-PC. The accuracy of the algorithms was evaluated on the basis of the coefficient of determination (R^2) of the linear fit and the root mean square error (RMSE) of pigment estimation.

Water sampling and analysis—Water samples (2 liters) for the calibration of the CASI imagery were collected from 13 stations on Barton Broad synchronous to the time frame of the 09:30 h NERC ARSF sortie. Water samples for image calibration were taken from the upper 0.3 m of the water column using an open-necked bottle. In addition, depth profiles were performed at three independent stations distributed across the lake. Water samples were extracted from depth using a pressurized discrete interval sampler (the data from these stations were not used for algorithm development). The need to sample the entire lake within the time frame of the NERC ARSF sorties unfortunately prevented depth profile sampling at further stations on the lake. In situ measurements of water temperature (°C) (near-surface layer only) and transparency (as the Secchi disc depth [SDD]) were made at each station. Further water samples for image calibration were also collected from three neighboring lakes of contrasting water quality (Hickling Broad, Horsey Mere, and Martham North Broad) that were encompassed by the NERC ARSF flight paths.

Water sample aliquots (250 mL) were filtered on to replicate Whatman GF/C filter papers and frozen at ≤80°C until analysis for Chl *a*, chlorophyll *b* (Chl *b*), chlorophyll c_{1+2} (Chl c_{1+2}), C-PC, and fucoxanthin could be performed. Chl *a* was dark-extracted in 90% acetone for 20 h, clarified by centrifugation (10 min; 5000 × g), and quantified spectrophotometrically according to the equations of Lorenzen and Jeffrey (1980). C-PC was extracted into a 50 mmol L^{-1} sodium phosphate buffer using probe sonication (1 min; 15-s bursts) and nine freeze–thaw cycles as described in Sarada et al. (1999). The extracts were clarified by centrifugation (10 min; 5000 × g) and the concentration of C-PC in the extracts was quantified using the spectrophotometric equations of Bennett and Bogorad (1973).

Chl *b*, Chl c_{1+2}, and fucoxanthin (biomarker pigments for chlorophytes and diatoms respectively) were determined using reversed-phase high performance liquid chromatography (RP-HPLC). The RP-HPLC system consisted of a Dionex quaternary pump connected to a Spherisorb™ OSD2 reverse-phase C-18 column and a Lab Alliance UV6000LP photodiode array detector (PDA). Pigments for RP-HPLC analysis were dark-extracted in 100% methanol for 20 h following sonication in an ice slurry for 1 min (in 15-s bursts) and clarified by centrifugation (10 min; 5000 ×

g) (Mantoura and Llewellyn 1983). 1 mol L^{-1} ammonium acetate v : v was added to the extract to serve as an ion-pairing agent to improve peak resolution and 100 μL of extract was manually injected into the RP-HPLC system. Pigments were separated at a flow rate of 1 mL s^{-1} using the linear gradient solvent system described in Wright et al. (1991). Pigment identification and quantification was performed against chlorophyll and carotenoid standards obtained from the Water Quality Institute (VKI), Hørsholm, Denmark, and via comparison to published elution sequences, retention times, and PDA spectra.

The concentration of total suspended particulate matter (SPM), suspended inorganic particulate matter (SPIM), and suspended organic particulate matter (SPOM) were determined gravimetrically. A sample aliquot (250 mL) was filtered onto prewashed and preweighed Whatman GF/C filter papers and SPM was determined by reweighing the filter after drying in an oven at 75°C for 12 h. The concentration of SPIM was subsequently determined by ashing the filter in a muffle furnace at 500°C for 24 h to remove the organic fraction. SPOM was determined as the difference in weight between SPM and SPIM.

Water chemistry and meteorological data—Water chemistry data for Barton Broad during 2005 were provided by England's Environment Agency (EA). This data included measurements of total phosphorus (TP) (PO_4-P), soluble reactive phosphorus (SRP) (PO_4-P), nitrite–nitrogen (NO_2-N), nitrate–nitrogen (NO_3-N), and ammonium–nitrogen (NH_4-N). The concentrations of total oxidized nitrogen (TON) (NO_2-N + NO_3-N), and dissolved inorganic nitrogen (DIN) (NH_4-N + NO_2-N + NO_3-N) were calculated from these measurements accordingly. Measurements of SPM, Chl *a*, SDD, the coefficient of diffuse attenuation of downward irradiance (K_d m^{-1}), lake surface temperature, and pH were also provided by the EA. Some limited phytoplankton cell counts during the *M. aeruginosa* bloom were also performed by the Broads Authority. All analyses were performed according to standard methods (Phillips and Kerrison 1991; Phillips et al. 2005). Meteorological data, including hourly wind and monthly rainfall measurements, from the nearest weather station (Coltishall, ~8 km) were provided by the United Kingdom's NERC British Atmospheric Data Centre.

Results

Seasonal trends in water quality—Seasonal trends in major physicochemical parameters in Barton Broad during 2005 are shown in Table 2 and Fig. 2. The concentration of Chl *a* increased from January to late May, with a brief clear-water period occurring between late May and mid-June. Chl *a* began to rapidly increase again from late June and reached an annual peak in late July (87.9 mg m^{-3}) coinciding with the peak of the *M. aeruginosa* bloom; Chl *a* remained high as the bloom persisted throughout August (68.4 mg m^{-3}) before slowly declining into late October (33.4 mg m^{-3}).

Seasonal trends in water transparency during 2005 were analogous to those of Chl *a*. The SDD was <1 m for the

Table 2. Seasonal trends in major water chemistry parameters in Barton Broad during 2005 (original data provided courtesy of the EA). TP and SRP are expressed as PO_4-P; the limit of detection for SRP was 0.5 $\mu g\ L^{-1}$.*

	TP ($\mu g\ L^{-1}$)	SRP ($\mu g\ L^{-1}$)	NH$_4$-N ($\mu g\ L^{-1}$)	NO$_3$-N ($\mu g\ L^{-1}$)	TON ($\mu g\ L^{-1}$)	DIN ($\mu g\ L^{-1}$)
31 Jan 05	15.5	1.4	30.3	117.0	121.6	151.8
11 Mar 05	13.2	≤0.5	3.9	115.3	118.3	122.3
26 Apr 05	7.9	≤0.5	21.2	67.5	71.0	92.2
10 May 05	8.9	≤0.5	23.6	91.2	100.9	124.5
23 May 05	8.9	≤0.5	35.7	65.1	70.2	105.9
28 Jun 05	9.9	≤0.5	18.2	9.3	12.8	30.9
22 Aug 05	21.1	≤0.5	22.4	10.7	12.6	35.0
24 Oct 05	14.2	1.3	34.5	57.3	64.5	99.0
08 Nov 05	18.5	1.2	36.9	66.1	74.0	110.9
21 Nov 05	9.8	3.9	58.1	96.0	104.3	162.4
14 Dec 05	10.8	1.7	72.0	ND	ND	ND
15 Dec 05	7.3	1.3	81.7	85.4	94.4	176.1

* TP, total phosphorus; SRP, soluble reactive phosphorus; TON, total oxidized nitrogen; DIN, dissolved inorganic nitrogen; ND, not determined.
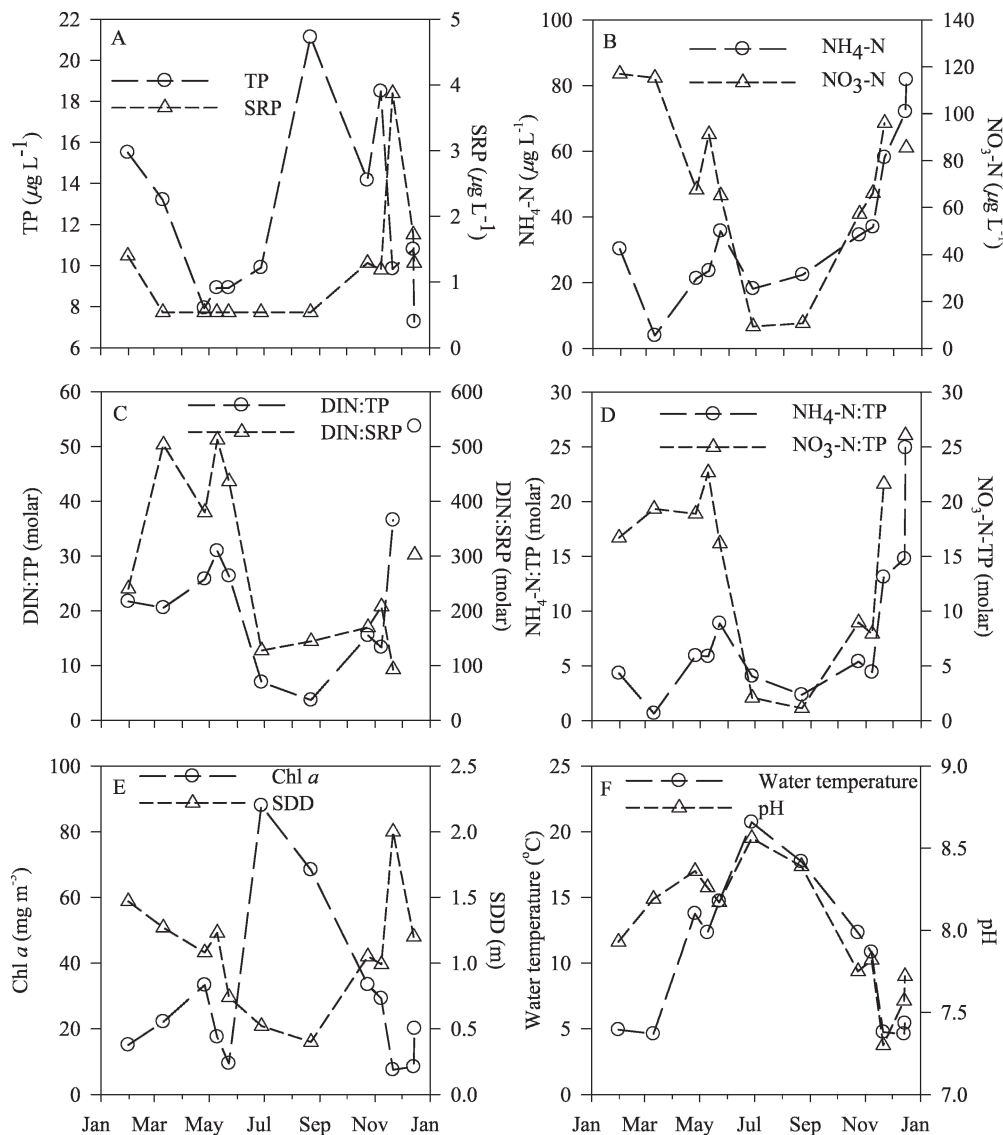

Fig. 2. Seasonal trends in water chemistry in Barton Broad: (A) TP and SRP; (B) NH$_4$-N and NO$_3$-N; (C) DIN : TP and DIN : SRP; (D) NO$_3$-N : TP and NH$_4$-N : TP; (E) Chl *a* and SDD; and (F) water temperature and pH. Grey area shows period in which the CASI-2 imagery of the *M. aeruginosa* bloom was acquired.
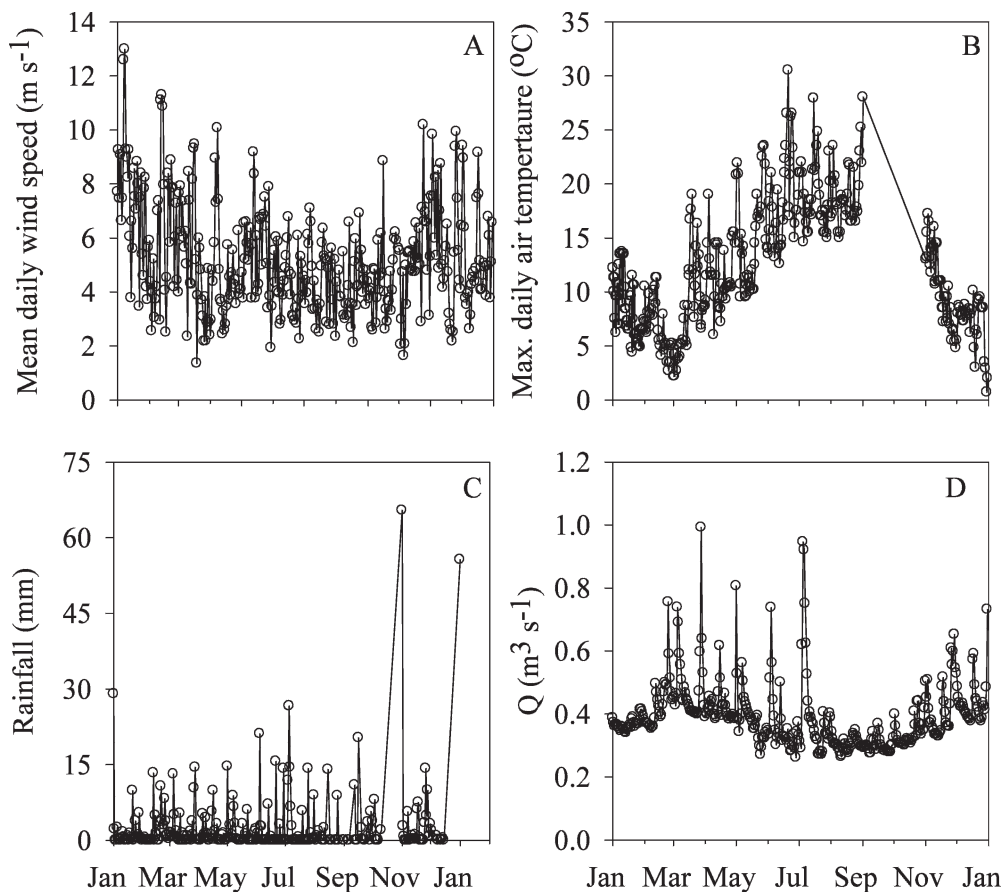
Fig. 3. Seasonal trends in the (A) mean daily wind speed, (B) maximum air temperatures, (C) rainfall, and (D) discharge on the River Ant for 2005. Weather observations were recorded at Coltishall (~8 km from Barton Broad). Grey area shows period in which the CASI-2 imagery of the *M. aeruginosa* bloom was acquired.

duration of the bloom and reached an annual minimum of 0.4 m in late July at the peak of the bloom. The concentration of TP increased from a late-April minimum (7.9 μg L^{-1}) to reach an annual peak during the bloom in August (21.1 μg L^{-1}); the concentration of SRP in Barton Broad was $\leq$0.54 μg L^{-1} from early March till late October. In similar fashion, the concentration of DIN decreased from a winter maximum of 151.8 μg L^{-1} to 30.9 μg L^{-1} during the bloom. The concentration of NH$_4$-N was lowest during March (3.93 μg L^{-1}) but significantly, in contrast to TON and DIN, increased to 22.4 μg L^{-1} during the bloom period in July and August.

The N : P (molar) ratio provides an indication of ambient nutrient stoichiometry for the bloom period. The water chemistry data show that during the bloom period the molar ratios of DIN : TP, DIN : SRP, and NO$_3$-N : TP decreased rapidly and reached annual minima of 3.7 : 1, 127 : 1, and 1.1 : 1 between July and late August respectively. NH$_4$-N : TP also decreased during the bloom period, reaching an annual minimum of 2.4 : 1 in late August, but it is notable that NH$_4$-N : TP did not decrease as markedly as did NO$_3$-N : TP.

The phytoplankton cell counts performed by the Broads Authority on 17 August 2005 and 25 August 2005 (12 and 4 d prior to the airborne sorties respectively) showed that

concentrations of *M. aeruginosa* in the open waters on 17 August 2005 were approximately 320 colonies mL^{-1} (no information on colony size was recorded). Dense surface scums were also noted in the vicinity of Neatishead (for clarification *see* Fig. 1). The samples collected on 25 August 2005 show that the concentration of *M. aeruginosa* had increased to 600 colonies mL^{-1} in the open waters, and concentrations >1000 colonies mL^{-1} were found in the waters around the boat yard at Barton Turf. During this period *M. aeruginosa* constituted approximately 90–95% of the total phytoplankton biomass.

Meteorological data for the bloom period indicate that the weather conditions were persistently warm and sunny weather (mean air temperature = 12.79°C [09:00 h GMT]; mean 6.6 h sunshine d^{-1}) with very moderate winds (mean wind speed = 3.48 m s^{-1}). Rainfall during the same period was low (29.8 mm). The only major rainfall event occurred on 15 August 2005 (14 mm), but this had a negligible effect on the hydrograph of the nearest gauging station on the River Ant. Discharge (Q) from River Ant into Barton Broad (measured at a gauging station 1.5 km upstream of the lake) was also low prior to the *M. aeruginosa* bloom (mean Q = 0.31 m^3 s^{-1}), which would suggest an absence of pronounced fluvial mixing and flushing (*see* Fig. 3).
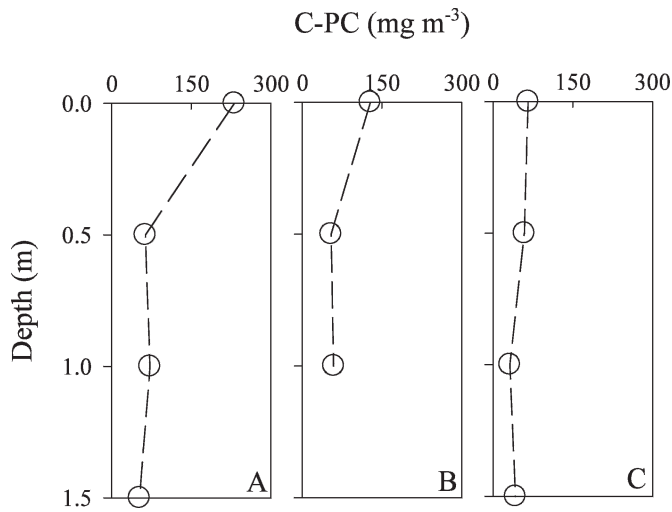
C-PC (mg m⁻³)

Fig. 4. (A–C) Depth profiles of the concentration of C-PC recorded at three discrete stations in Barton Broad on 29 August 2005.

Airborne remote sensing of bloom dynamics—The mean concentration of Chl *a* in the water samples collected from the 13 stations on Barton Broad contemporaneous to the 09:30 h GMT NERC ARSF sortie on 29 August 2005 was (mean ± 2 SE) 45.8 ± 8.0 mg m⁻³ ($n = 13$). The mean concentration of C-PC was 79.2 ± 29.7 mg m⁻³. The mean concentrations of the other taxonomically significant accessory pigments were Chl *b* = 8.2 ± 1.8 μg L⁻¹, Chl c_{1+2} = 2.3 ± 0.7 μg L⁻¹, and fucoxanthin = 9.8 ± 2.3 μg L⁻¹. The accessory pigment to Chl *a* ratios were Chl *b* : Chl *a* = 0.09 ± 0.01, Chl c_{1+2} : Chl *a* = 0.05 ± 0.01, fucoxanthin : Chl *a* = 0.26 ± 0.06, and C-PC : Chl *a* = 2.29 ± 0.78. High concentrations of SPM were also recorded. Total SPM = 48.6 ± 7.2 mg L⁻¹, SPIM = 28.5 ± 5.5 mg L⁻¹, and SPOM = 20.1 ± 1.9 mg L⁻¹. The mean SDD = 0.43 ± 0.02 m.

The depth profiles of C-PC measured at three independent stations appear to show some variation in vertical distribution of cyanobacterial biomass (Fig. 4). The depth profile depicted in Fig. 4A (collected from a station in the north of Barton Broad) shows higher C-PC concentrations towards the water surface—indicative of near-surface accumulations of buoyant cyanobacteria. A similar trend can also be observed in Fig. 4B, which shows the depth profile for a mid-lake station. In contrast, the depth profile of C-PC depicted in Fig. 4C obtained from a station in the south of Barton Broad demonstrates more vertical homogeneity with depth.

The $\log_{10}$-transformed least-squares regression analyses between the band ratios and the measured pigment concentrations are depicted in Fig. 5. The derived semiempirical algorithm for Chl *a* (Eq. 1) yielded $R^2 = 0.960$ ($n = 13$, $p < 0.001$, RMSE = 7.07 mg m⁻³) and the semiempirical algorithm for C-PC (Eq. 2) yielded $R^2 = 0.947$ ($n = 13$, $p < 0.001$, RMSE = 11.9 mg m⁻³) for the fit against measured pigment concentrations (for clarity, the RMSE is reported on the linear scale).
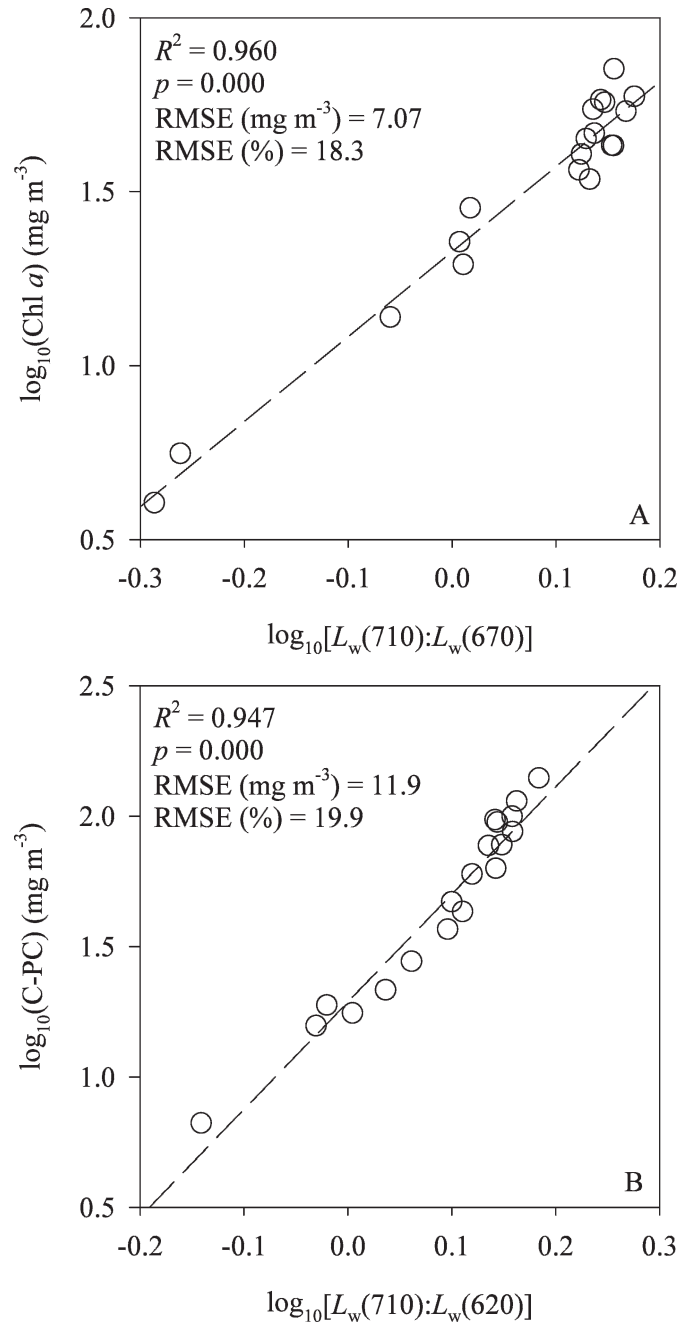
Fig. 5. The optimum $\log_{10}$-transformed CASI-2 water-leaving radiance retrieval algorithms for (A) Chl *a* and (B) C-PC.

$$\log_{10}(\text{Chl } a)(\text{mg m}^{-3}) = 1.33 + 2.44 \times \log_{10}[L_w(710) : L_w(670)] \tag{1}$$

$$\log_{10}(\text{C} - \text{PC})(\text{mg m}^{-3}) = 1.29 + 4.12 \times \log_{10}[L_w(710) : L_w(620)] \tag{2}$$

A degree of nonlinearity can be observed in the plotted function for C-PC (Fig. 5B). This nonlinearity may have been caused by the increasing saturation of the [L_w(710)

Fig. 6. Time-series CASI-2 images depicting changes in the distribution of C-PC in Barton Broad on 29 August 2005 at (A) 16:00 h GMT, (B) 09:30 h GMT, and (C) 12:00 h GMT.
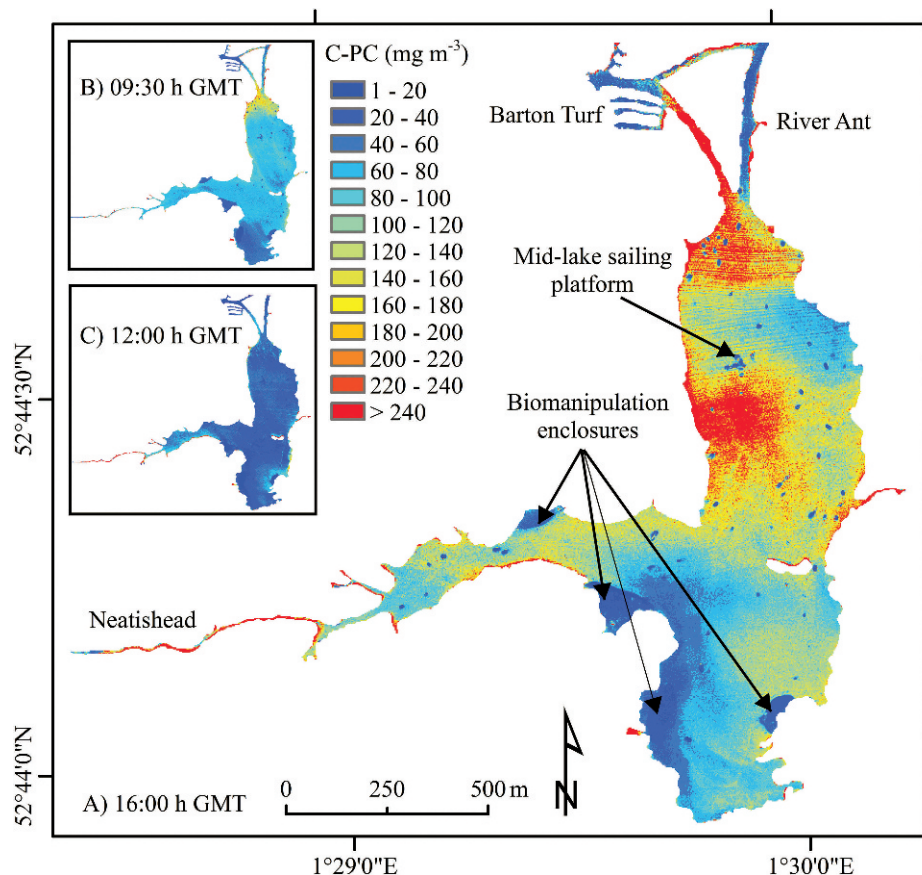
: $L_w(620)$] band ratio at high C-PC concentrations (i.e., >80 mg m^{-3}). The use of a second-order polynomial function provided a slight improvement in the R^2 and RMSE of the log–log fit between [$L_w(710):L_w(620)$] and measured C-PC. However, a linear fit was preferred in this instance, because it essentially provided a more conservative estimate of pigment concentrations where $\log[L_w(710):L_w(620)]$ exceeded the range over which the algorithm was derived (i.e., >log(1.5)) and thus reduced uncertainty in image interpretation.

The calibrated CASI-2 time-series images of diurnal change in the C-PC concentration in the surface waters of Barton Broad are shown in Fig. 6. The calibrated CASI-2 time-series images of diurnal change in the Chl *a* concentration, and the image-derived C-PC:Chl *a* ratio, are shown in Fig. 7. The CASI-2 images clearly show that significant distributional changes occurred in the concentrations of both C-PC and Chl *a* during the time frame of image acquisition on 29 August 2005. The statistics for these calibrated images are detailed in Table 3. The measured and image-derived mean near-surface concentrations of both C-PC and Chl *a* in the lake at 09:30 h GMT demonstrated good agreement. The lowest image-derived mean concentrations of both C-PC and Chl *a* were observed at 12:00 h GMT (39.7 mg C-PC m^{-3} and 23.6 mg Chl *a* m^{-3}); the near-surface concentrations of both C-PC and Chl *a* then increased rapidly to a maximum

at 16:00 h GMT (112.9 mg C-PC m^{-3} and 54.3 mg Chl *a* m^{-3}). Intermediate concentrations of C-PC and Chl *a* were observed at 09:30 GMT (74.4 mg C-PC m^{-3} and 48.9 mg Chl *a* m^{-3}). The percentage increases in the near-surface concentrations of C-PC and Chl *a* from the 12:00 h GMT minimum to the 16:00 h GMT maximum were thus 184% and 130% respectively.

The standard deviation (*s*) provides an indication of the spatial variability in the near-surface concentrations of Chl *a* and C-PC over the image time series. Spatial variability in the concentrations of C-PC and Chl *a* was minimal at 12:00 h GMT (*s* = 20.7 mg C-PC m^{-3} and 9.4 mg Chl *a* m^{-3}), but maximal at 16:00 h GMT (*s* = 49.3 mg C-PC m^{-3} and 18.3 mg Chl *a* m^{-3}). Again, intermediate spatial variability in pigment concentrations was observed at 09:30 h GMT (*s* = 26.8 mg C-PC m^{-3} and 11.5 mg Chl *a* m^{-3}). In the 09:30 h GMT and 16:00 h GMT Chl *a* and C-PC calibrated images, discernible near-surface aggregations of *M. aeruginosa* can be observed around the northern shore, and, in the case of the 16:00 h GMT image, near-surface aggregations can be observed in the vicinity of the mid-lake sailing platform. High near-surface concentrations were also visible throughout the day in the western arm of the lake. The effect of these near-surface aggregations on the mean and *s* of the pigments is shown in Fig. 8.

The CASI-2 images of C-PC and Chl *a* in Barton Broad clearly show that the *M. aeruginosa* bloom underwent
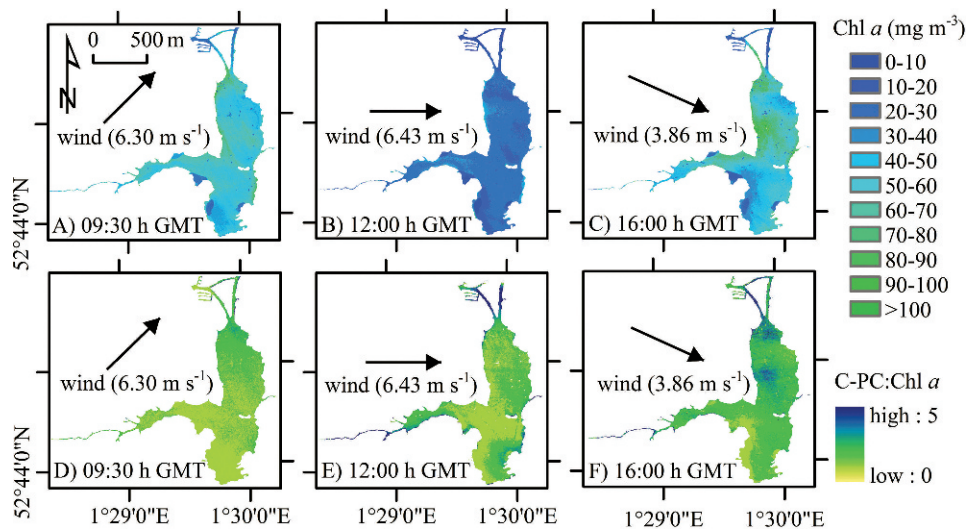
Fig. 7. Time-series CASI-2 images depicting changes in the distribution of (A–C) Chl *a* and (D–F) C-PC:Chl *a* in Barton Broad on 29 August 2005 at 09:30 h, 12:00 h, and 16:00 h GMT.

considerable restructuring throughout the course of the day. This view is further reinforced by the image-derived C-PC:Chl *a* ratios, which provide a relative index of cyanobacterial abundance (Fig. 7) (Ahn et al. 2002). In Fig. 7, high C-PC:Chl *a* ratios can be seen towards the northern shore of the lake at 09:30 h GMT, with lower C-PC:Chl *a* ratios occurring towards the southern shore. This pattern changes slightly by 12:00 h GMT, with higher C-PC:Chl *a* ratios observed towards the eastern shore. High C-PC:Chl *a* ratios can again be observed in the north of the lake at 16:00 h GMT, but with large mid-lake patches of high C-PC:Chl *a* occurring in the vicinity of the sailing platform. The accessory pigment to Chl *a* ratios measured at each station on Barton Broad at 09:30 h GMT are depicted in Fig. 9. The accessory pigment ratios show a clear trend of higher C-PC:Chl *a* (higher cyanobacterial abundance) towards the northern and leeward shore with higher fucoxanthin:Chl *a* ratios (likely to be indicative of higher diatom abundance) in the mid and southern parts of the lake.

The diurnal change in the spatial distribution of C-PC, Chl *a*, and C-PC:Chl *a* also demonstrated a reasonable

association with the prevailing wind direction for each time-series CASI-2 image. It is also notable that the mean wind speed at 09:30 h GMT (6.30 m s^{-1}) and 12:00 h GMT (6.43 m s^{-1}) was significantly higher than that recorded at 16:00 h GMT (3.86 m s^{-1}) (Fig. 10).

Discussion

Development and persistence of the bloom—Blooms of cyanobacteria have been a common occurrence in Barton Broad over recent decades. Typically, these blooms have been dominated by the oscillatorians *P. agardhii* and *L. redekei* (functional group S) (Reynolds et al. 2002), largely because these species are well-adapted to growth in shallow, turbid, and well-mixed lakes. Blooms of dinitrogen-fixing cyanobacteria have also occurred intermittently (*Anabaena* spp. and *A. flos-aquae*—functional group H1). However, the occurrence of cyanobacteria blooms in Barton Broad has declined following the implementation of lake restoration measures (Phillips et al. 2005). Indeed, the cyanobacterial bloom observed in the summer of 2005 was the first to develop for several years. Moreover, it was

Table 3. The measured and image-derived concentrations of C-PC and Chl *a* in Barton Broad on 29 August 2005 at 09:30, 12:00, and 16:00 h GMT.*

	Measured		Image-derived					
	C-PC (mg m^{-3})	Chl *a* (mg m^{-3})	C-PC (mg m^{-3})			Chl *a* (mg m^{-3})		
	09:30 h	09:30 h	09:30 h	12:00 h	16:00 h	09:30 h	12:00 h	16:00 h
n	13	13	107,959	107,193	106,552	107,959	107,193	106,552
Min	36.62	34.16	0.79	0.09	0.47	7.84	1.46	1.83
Max	138.76	70.88	249.61	249.73	249.92	249.86	249.5	249.28
Mean	79.20	49.18	74.40	39.70	112.86	48.90	23.56	54.32
SD	29.66	10.51	26.77	20.66	49.26	11.53	9.38	18.25
SE	8.23	2.91	0.081	0.063	0.151	0.035	0.029	0.056
C.V.	0.37	0.21	0.36	0.52	0.44	0.24	0.40	0.34

* C-PC, C-phycocyanin; Chl *a*, chlorophyll *a*; Min, minimum; Max, maximum.
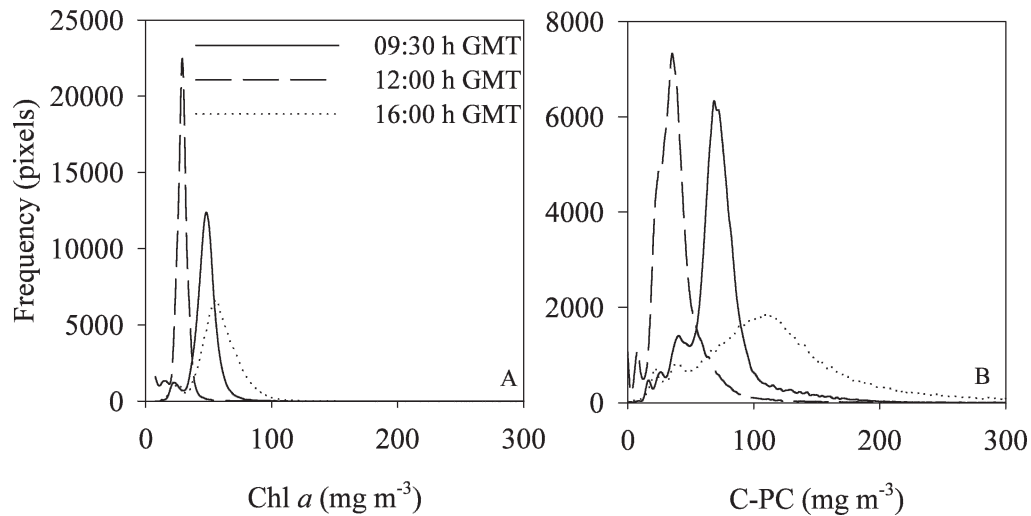
Fig. 8. Histograms showing the changes in the statistical distribution of near-surface concentrations of (A) Chl *a* and (B) C-PC at 09:30 h, 12:00 h, and 16:00 h GMT in Barton Broad on 29 August 2005.

also the first recorded incidence of an *M. aeruginosa* (functional group L_M) bloom on the lake (A. Kelly pers. comm.).

This suggests that the phytoplankton assemblage of Barton Broad is continuing to respond, perhaps somewhat hysteretically, to lake restoration measures. The floristic responses of phytoplankton communities to nutrient reduction are not well documented; the factors that

contributed to the development and persistence of the *M. aeruginosa* bloom on Barton Broad are therefore of some interest. The seasonal Chl *a* data indicate that the *M. aeruginosa* bloom began to develop during late June and July and persisted until at least early September. The C-PC concentration measured on 22 June 2005 was 17.73 ± 5.73 mg m^{-3} and the C-PC:Chl *a* ratio was <0.5; these values are significantly lower than the C-PC concentration
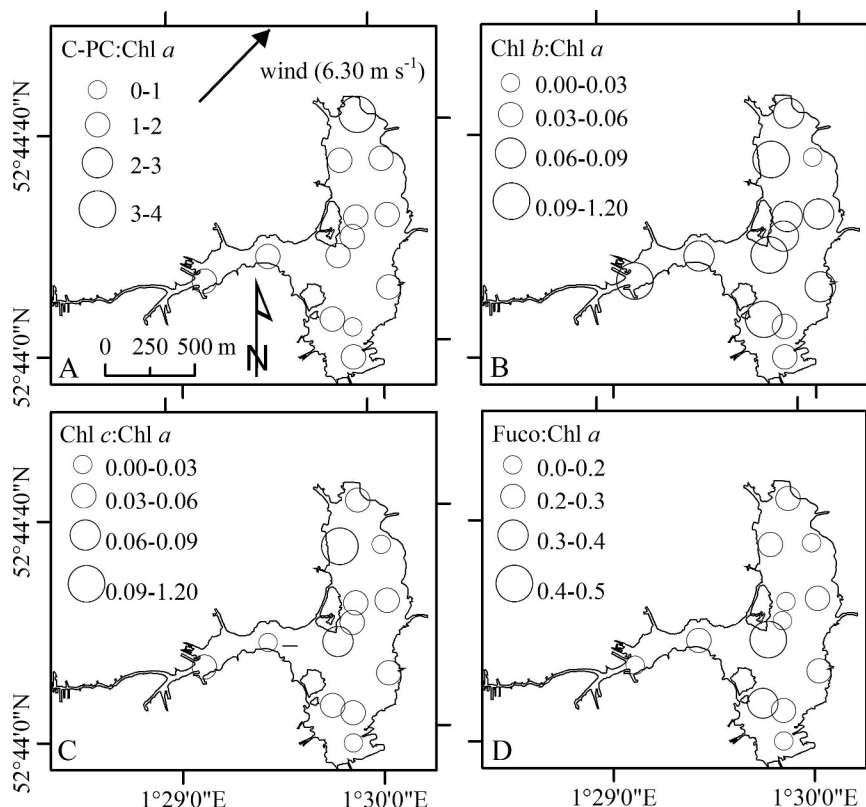

Fig. 9. Spatial variations in pigment ratios measured on Barton Broad on 29 August 2005 at 09:30 h GMT. (A) C-PC:Chl *a*, (B) Chl *b*:Chl *a*, (C) Chl *c*:Chl *a*, and (D) Fucoxanthin:Chl *a*.
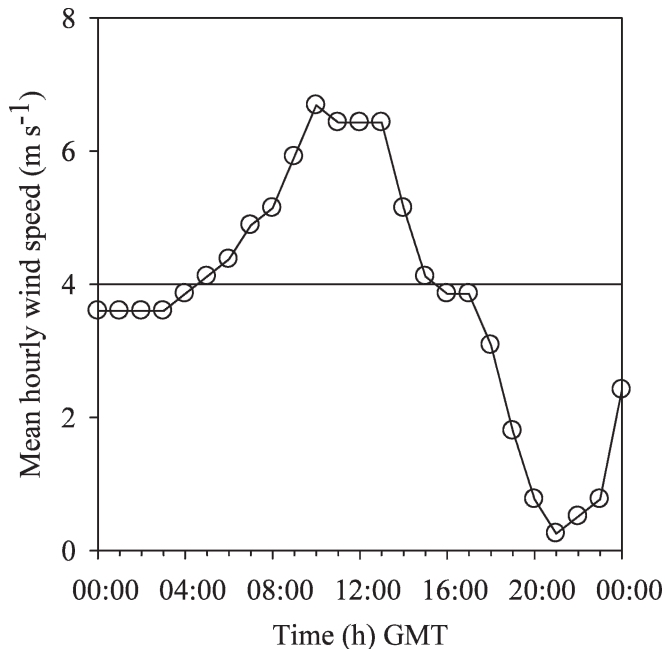
Fig. 10. Hourly changes in the mean wind speed on 29 August 2005. Observations were recorded at Coltishall (~8 km from Barton Broad). Solid line indicates 4 m s^{-1} threshold.

(79.2 $\pm$ 29.7 mg m^{-3}) and C-PC : Chl a ratio (2.29 $\pm$ 0.78) measured at the peak of the bloom in late August. This suggests that *M. aeruginosa* (and other cyanophytes) were subdominant or codominant in late June. The rapid increase in the Chl a concentration observed in early July following the brief clear-water phase therefore likely reflects the increasing dominance of *M. aeruginosa*.

This increase in cyanobacterial biomass coincided with the acute depletion of dissolved nutrient pools (DIN and SRP). It is notable that the TON pool began to rapidly deplete immediately prior to the *M. aeruginosa* bloom, and this depletion accelerated as the bloom persisted. Many cyanobacteria species have a lower optimum N : P ratio for growth than eukaryotic phytoplankton and are thus generally favored during periods of N depletion (Dokulil and Teubner 2000). It is also significant that the diminution of the NH$_4$-N pool was not as pronounced as that of NO$_3$-N. It has been suggested that the depletion of NO$_3$-N particularly favors cyanobacteria, because they have a greater preference and superior uptake kinetics for NH$_4$-N and can thus outcompete eukaryotic phytoplankton for limited NH$_4$-N reserves under NO$_3$-N stress (Hyenstrand et al. 1998; Dokulil and Teubner 2000). McQueen and Lean (1987) have suggested that a NO$_3$-N : TP ratio <5 : 1 (by mass) favors cyanobacteria dominance; the NO$_3$-N : TP ratios (by mass) in Barton Broad were 0.5–0.9 : 1 from late June till late August. The near-exhaustion of the NO$_3$-N pool is therefore likely to have increased selection pressure for cyanobacterial dominance.

Despite the acute depletion of TON, the lake was unlikely to be N-limited during the summer of 2005, because the near-constant NH$_4$-N concentrations shown in Fig. 2 suggest that ammonium was being efficiently recycled. In the absence of a substantial ambient pool, rapid NH$_4$-N turnover can be sufficient to maintain large standing crops of cyanobacteria (Humphries and Lyne 1988), and this is likely to have been a major factor behind the persistence of the *M. aeruginosa* bloom. Although DIN : TP (3.7 : 1) was below the Redfield ratio, the stoichiometry of the immediately bioavailable fractions— DIN : SRP (144 : 1) and NH$_4$-N : SRP (92 : 1)—would seem to suggest that the heavily deleted SRP pool may have been more limiting to growth, particularly if NH$_4$-N was being efficiently recycled.

Unlike eukaryotic algae, cyanobacteria can accumulate and store phosphorus as an intracellular reserve and are therefore less dependent on external nutrition during periods of P stress. Furthermore, *M. aeruginosa* has a high affinity for phosphorus and thus retains greater fitness for episodically SRP-depleted environments than many other cyanophytes (Dokulil and Teubner 2000; Reynolds 2006). Thus, the ability to compete for limited SRP resources may have also been an important factor in the development and persistence of the *M. aeruginosa* bloom. In addition, the ability of *M. aeruginosa* to compete through the production of toxins may also have been a significant factor, although we have no data on toxin production during the bloom to substantiate this (Lindholm et al. 1989; Boon et al. 1994).

The hydrodynamic conditions in Barton Broad during late July and August were also favorable for cyanobacteria. The weather was very warm and a lack of significant rainfall reduced fluvial throughput from the River Ant, which would suggest that the lake endured a period of reduced flushing and weakened fluvial mixing. Populations of buoyancy-regulating cyanobacteria are prone to losses incurred from flushing, and thus this period of relatively insipid weather may have been vital to the development of the bloom. Hydrodynamic stability may also explain the dominance of *M. aeruginosa* over other bloom-forming cyanobacteria that were previously more common in the lake. *P. agardhii* and *L. redekei* are well-adapted to highly light-deficient environments, but these species are reliant on well-mixed conditions to ensure sufficient insolation in turbid lakes. In contrast, *M. aeruginosa* is sensitive to low ambient light (Reynolds et al. 2002; Havens et al. 2003), but it can escape light starvation by migrating to better illuminated near-surface waters. As the restoration of Barton Broad has resulted in significant improvements in the ambient light climate (Phillips et al. 2005), this will certainly have favored *M. aeruginosa* over the more shade-tolerant *P. agardhii* and *L. redekei*.

Nevertheless, the light climate in Barton Broad during the mid- and late-summer bloom season remains poor (Phillips et al. 2005). Thus, for the *M. aeruginosa* bloom to persist under such conditions, it would have been vital that colonies were able to migrate and maintain a station in near-surface waters. However, it can be argued that in a well-mixed fluvial lake such as Barton Broad, the ability of *M. aeruginosa* to form near-surface aggregations may be limited. This therefore raises important questions concerning the efficacy of buoyancy regulation by *M. aeruginosa* in polymictic shallow lakes, and its role in facilitating the persistence of blooms.

Spatial dynamics of the bloom—The presumption that *M. aeruginosa* colonies were able to undertake passive migrations to near-surface waters is clearly supported in the time-series CASI-2 images. The images show that marked changes in the near-surface concentrations of Chl *a* and C-PC in Barton Broad occurred between 09:30 h and 16:00 h GMT. Vertical migration in cyanobacteria often demonstrates a pronounced diel pattern because of the close association between carbohydrate-mediated cell buoyancy and photosynthetic activity during the photoperiod (Oliver 1994). Near-surface accumulations of *M. aeruginosa* colonies are clearly evident in the 09:30 h GMT image. This is consistent with previous studies that have shown that buoyant colonies nocturnally migrate and amass in near-surface waters during the hours of darkness (Reynolds and Rogers 1976; Takamura and Yasuno 1984; Visser et al. 1996). On this basis, the 09:30 h GMT CASI-2 images would seem to depict the remnants of nocturnal scums. The in situ depth profiles measured during the course of the lake sampling provide an image-independent verification that near-surface accumulations of *M. aeruginosa* colonies were initially present in Barton Broad at 09:30 h GMT, particularly in the north of the lake.

It is notable that these near-surface accumulations appear to have dispersed in the 12:00 h GMT CASI-2 Chl *a* and C-PC images. This observation is again coherent with previous work, which has shown that the high insolation incurred by colonies stationed in near-surface waters drives the photosynthetic production of high-molecular-weight polymers (e.g., glycogen), which increases colony density sufficiently to induce sinking to deeper horizons (Kromkamp et al. 1988; Oliver 1994).

Several workers have observed that the formation of near-surface accumulations of buoyant cyanobacteria is dependent on the extent of water column turbulence. George and Edwards (1976) suggest that wind speeds in excess of ~ 4 m s^{-1} are sufficient to induce turbulent mixing in shallow lakes and suppress upwards migrations by buoyant cyanobacteria. The wind speed between 00:00 h and 06:00 h GMT was ~ 4 m s^{-1}; this then increased to >6 m s^{-1} by 09:30 h GMT. Therefore, the dispersion of the early-morning near-surface scums was probably facilitated appreciably by more pronounced wind-induced mixing. This is consistent with the findings of Cao et al. (2006), who noted that near-surface aggregations of *M. aeruginosa* in Lake Taihu (People's Republic of China) were only observed during periods when the wind speed was <4 m s^{-1}.

The 16:00 h GMT CASI-2 Chl *a* and C-PC images again show clear evidence of near-surface accumulations of *M. aeruginosa* colonies. In this instance, the image-derived near-surface Chl *a* and C-PC concentrations were even higher than those observed at 09:30 h GMT. Thus, it appears that the *M. aeruginosa* colonies had recovered sufficient buoyancy from the morning to migrate and maintain station in near-surface waters. These migrations may have been facilitated by the depletion of photosynthate reserves while colonies were immersed in deeper and more turbid horizons earlier in the day. However, it must also be noted that the wind speed at 16:00 h GMT had fallen to

<4 m s^{-1}, which implies a reduction in the degree of turbulent mixing and increased water column stability.

This increased water column stability would have been essential to enable colonies to migrate back to near-surface waters. Indeed, it is difficult to determine the extent to which the accretion of *M. aeruginosa* in near-surface waters was the result of buoyancy regulation or the response of continuously positively buoyant colonies to changes in water column turbulence. If conditions permit, *M. aeruginosa* can remain positively buoyant for several days (Reynolds 1973; Humphries and Lyne 1988); this is advantageous because it enables colonies in shallow waters to rapidly recover an optimum station following disturbance (e.g., wind-induced mixing). Thus, given the rate at which colonies appear to have returned to near-surface waters in the late afternoon, it is possible that colonies remained positively buoyant, with the near-surface accumulations forming rapidly during periods without significant wind-induced mixing (i.e., immediately prior to 09:30 h and 16:00 h GMT). Near-surface accumulations of *M. aeruginosa* visible in the western arm of the lake throughout the day support the view that (at least some) colonies remained positively buoyant. The observed vertical restructuring of the bloom would therefore seem to be largely driven by wind-induced mixing.

The effect of wind-induced hydraulic circulation on the horizontal distribution of phytoplankton in lakes has also been well documented (George and Edwards 1976; Webster 1990). The importance of wind speed and direction in determining the horizontal distribution of *M. aeruginosa* colonies in Barton Broad is clearly evident in the CASI-2 images of the C-PC : Chl *a* ratio. The spatial patterns in the C-PC : Chl *a* images show good agreement with the prevalent wind direction throughout the duration of the morning. Aggregations of *M. aeruginosa* can be observed towards the northern leeward shore of Barton Broad at 09:30 h GMT and the eastern leeward shore at 12:00 h GMT (Fig. 7). This clearly demonstrates that the horizontal restructuring of blooms of buoyant cyanobacteria in response to changes in the prevalent wind direction can be very rapid.

The measured C-PC : Chl *a* ratios also show evidence of high concentrations of *M. aeruginosa* towards the northern leeward shore at 09:30 GMT (Fig. 7), which substantiates the patterns observed in the CASI-2 imagery. It has been shown that during periods of advective circulation, negatively buoyant phytoplankton often tend to aggregate towards the windward shore, as cells become entrained within subsurface return flows and accumulate in regions of upwelling water (George and Edwards 1976; Hedger et al. 2004). Therefore, the higher fucoxanthin : Chl *a* ratios measured at sampling stations in the mid and southern regions of the lake may indicate that negatively buoyant eukaryotic phytoplankters (likely diatoms) were being transported towards the southern windward shore.

Very shallow lakes such as Barton Broad are typically well mixed, and this promotes homogeny in the distribution of phytoplankton. However, the CASI-2 time-series images show that the formation of near-surface accumulations in Barton Broad by buoyant *M. aeruginosa* colonies was

highly spatially variable, even during those periods where wind-induced turbulence increased. It would appear that the complex nearshore morphometry of Barton Broad creates several regions of sheltered water where wind-induced (or even fluvially induced) mixing is less pronounced. The time-series CASI-2 imagery shows that the formation of near-surface accumulations in Barton Broad was most marked in these more stagnant regions. In the more sheltered western arm of the lake, it is notable that near-surface accumulations were able to persist to some extent throughout the day. Furthermore, it is notable that the most pronounced near-surface accumulations observed in the 16:00 h GMT CASI-2 images occurred in proximity to the mid-lake sailing platform and in the waters surrounding the harbor at Barton Turf. It is likely that the sailing platform suppresses turbulence in adjacent waters, therefore promoting sufficient water column stability to harbor dense near-surface aggregations of *M. aeruginosa*. The waters that surround the harbor at Barton Turf are also highly stagnant and it is therefore not unexpected that heavy surface scums of *M. aeruginosa* were also observed in this region.

Blooms of cyanobacteria are generally considered to be indicative of poor ecological status. However, it could be argued that the unprecedented blooms of shade-intolerant *M. aeruginosa* are actually indicative of a recovery in the water quality status of Barton Broad, particularly the ambient light climate. Nevertheless, water column stability is important for the growth of *M. aeruginosa* (Reynolds and Walsby 1975; Reynolds et al. 2002). In Barton Broad, refuges of stable water may have been important in creating a series of locales in which *M. aeruginosa* colonies could continually occupy a station favorable to growth. Zohary and Breen (1989) have previously remarked that lake morphology is important to the formation of *M. aeruginosa* scums. In this respect, the effect of lake morphology on migrational behavior may also influence the persistence of cyanobacterial blooms in shallow lakes such as Barton Broad.

Remote sensing of cyanobacterial blooms—The derived CASI-2 water-leaving radiance band ratios $[L_w(710):L_w(670)]$ and $[L_w(710):L_w(620)]$ both demonstrated excellent relationships with the measured concentrations of Chl *a* and C-PC respectively ($R^2 \geq 0.95$; RMSE < 20%) in log–log space. This further demonstrates that remote sensing is an effective tool for monitoring cyanobacterial blooms in lakes. In this study, because we were not interested in estimating the concentration of C-PC in other lakes beyond Barton Broad, and the intention was not to derive operational algorithms for the estimation of Chl *a* or C-PC, a simple semiempirical approach using a dark-pixel approximation of $L_w(\lambda)$ was considered sufficient.

The semiempirical approach for the estimation of C-PC assumes that absorption at 620 nm can be attributed entirely to C-PC. However, this is not strictly correct, because Chl *a* also absorbs light in the 620 nm region (although significantly less so than C-PC per unit concentration). The accuracy of the semiempirical approach is therefore inherently susceptible to variability in

the C-PC:Chl *a* ratio. Consequently, C-PC may be overestimated where the C-PC:Chl *a* ratio is low (i.e., in floristically mixed phytoplankton assemblages). We found a positive association between the standardized residual values on the estimation of C-PC and the C-PC:Chl *a* ratio ($n = 13$, $R^2 = 0.453$, $p = 0.016$); this suggests that some of the error on the estimation of C-PC was the result of variability in the C-PC:Chl *a* ratio. However, because the values of both the C-PC concentration (43–139 mg m^{-3}) and the C-PC:Chl *a* ratio (0.96–3.25) were high, the effect of these errors on the accuracy of the C-PC estimation was minimal in this instance.

Simis et al. (2005) propose a semianalytical algorithm for the estimation of C-PC that incorporates an empirically derived correction factor (ε) for absorption at 620 nm by Chl *a*, such that the accuracy of the algorithm is not as dependent on stability in the C-PC:Chl *a* ratio. This approach would seem to offer a way forward in lakes where the C-PC:Chl *a* ratio may vary significantly. However, Simis et al. (2005) found that errors in the estimation of C-PC were still incurred where cyanobacteria were not the dominant floristic component of the phytoplankton community (e.g., C-PC:Chl *a* < 0.4), partly because ε was derived only for cyanobacteria-dominated waters.

In addition, Simis et al. (2007) show that the coincidental presence of other accessory pigments that absorb light in proximity to the 620 nm region (e.g., Chl *b* and Chl c_{1+2}) can also result in errors in the estimation of C-PC. We also found a significant relationship between the standardized residuals from our C-PC algorithm and the measured concentration of Chl *b* ($n = 13$, $R^2 = 0.367$, $p = 0.028$) (although not with Chl c_{1+2}). Therefore, a degree of caution is necessary when the concentration of C-PC is to be estimated using either semiempirical or semianalytical methods in waterbodies where other eukaryotic algae species form a significant component of the phytoplankton assemblage. It is clear that further work should be focused on improving the accuracy of C-PC estimation in floristically mixed phytoplankton assemblages.

The remote-sensing–based estimation of C-PC is also prone to errors where variability occurs in the specific absorption coefficient of C-PC ($a^*_{CPC}(620)$), which can arise because of pigment packaging effects and photoadaptive responses. The intracellular C-PC content of cyanobacteria can also vary considerably between different species. In addition, the intracellular concentration of C-PC in cyanobacteria is highly dependent on physiological status. For example, under N-replete conditions cyanobacteria may manufacture excess C-PC as an N storage product. In contrast, under N-depleted conditions cyanobacteria may break down C-PC to use as an N source (Boussiba and Richmond 1980).

The diurnal patterns in the concentration of cyanobacterial pigments in the near-surface layer of Barton Broad could also be explained by such changes in the intracellular pigment content of *M. aeruginosa*. However, it is very doubtful that changes of such magnitude and direction in the C-PC content of *M. aeruginosa* would occur over a relatively short space of time under natural conditions. Moreover, because similar diurnal patterns were observed

in the concentration of Chl *a*, whose concentration does not fluctuate as rapidly at the intracellular level, it would seem reasonable to conclude that the observed changes in near-surface pigment concentrations were the result of the vertical and horizontal restructuring of the bloom. Nevertheless, further research is also needed to examine the reliability of C-PC as a quantitative biomarker of cyanobacterial abundance for different cyanobacteria genera under varying levels of physiological stress.

Radiance reflected from bottom sediments can have a significant influence on water-leaving radiance in optically shallow waters, and this can lead to substantial errors in remotely sensed pigment concentrations (Cannizzaro and Carder 2006). However, this is unlikely to have been a significant factor in this study, because the transparency of the water column in Barton Broad was very poor (for example, K_d was $>3.30 \text{ m}^{-1}$ in June, and SDD was ≤ 0.45 m in both June and August). Therefore, upwelling radiance from the lake bed is likely to have been low, particularly because the bottom sediments of the Norfolk Broads tend to be largely composed of organic detritus (Hunter et al. 2008). Moreover, because the lake has a flat-bottomed bathymetry, any bottom radiance effect is likely to be relatively uniform across the lake.

The routine monitoring of cyanobacterial blooms in inland or coastal waters will require the development of operational algorithms for the retrieval of Chl *a* and C-PC using current and future satellite sensors. The much-proclaimed ability of remote sensing to provide early-warning risk monitoring of toxic cyanobacterial blooms in lakes will demand low detection limits for C-PC. The World Health Organization (WHO) guidelines values suggest that a low risk of short-term mild illnesses may occur from exposure to toxins where cyanobacteria occur at concentrations of approximately 20,000 cells mL^{-1} (approximately equivalent to 10 mg Chl *a* m^{-3}) (WHO 2003). Metsamaa et al. (2006) have suggested that the diagnostic absorption feature at 620 nm associated with C-PC can be observed at a Chl *a* concentration of c. 8–10 mg m^{-3} in the Baltic Sea. On this basis, assuming that comparable detection limits for C-PC can be attained in turbid inland waters, it would seem that remote sensing could be used for early-warning monitoring of potentially toxic cyanobacterial blooms in lakes. However, a better understanding of the detection limits for C-PC in inland waters is clearly required, particularly at the early stages of blooms, when cyanobacteria may be subdominant to eukaryotic algae.

In summary, we show that airborne remote sensing can be used to provide high-resolution time-series reconnaissance of diurnal vertical migration by cyanobacterial blooms. The CASI-2 time-series images show that localized vertical migrations by buoyancy-regulating cyanobacteria can create pronounced patchiness in the spatial distribution of phytoplankton blooms, particularly in lakes with complex hydrodynamics. This patchiness was highly transient and responded rapidly to changes in the physical conditions and, in particular, wind-induced mixing and circulation. This is the first time such behavior has been examined at the lake scale, and these spatially explicit insights into bloom behavior could not have been obtained without the use of remote sensing reconnaissance. Although we focused specifically on vertical migration in a small freshwater lake, because cyanobacteria also exhibit similar behavior in deep lakes, coastal waters, and even in the open oceans, remote sensing could equally be used to study the vertical dynamics of cyanobacteria populations in these environments.

References

AHN, C. Y., A. S. CHUNG, AND H. M. OH. 2002. Rainfall, phycocyanin, and N : P ratios related to cyanobacterial blooms in a Korean large reservoir. Hydrobiologia **474:** 117–124.

BENNETT, A., AND L. BOGORAD. 1973. Complementary chromatic adaptation in a filamentous blue-green-alga. J. Cell Biol. **58:** 419–435.

BOON, P. I., S. E. BUNN, J. D. GREEN, AND R. J. SHIEL. 1994. Consumption of cyanobacteria by fresh-water zooplankton—implications for the success of top-down control cyanobacterial blooms in Australia. Aust. J. Mar. Freshw. Res. **45:** 875–887.

BOUSSIBA, S., AND A. E. RICHMOND. 1980. C-phycocyanin an a storage protein in the blue-green-alga *Spirulina platensis*. Arch. Microbiol. **125:** 143–147.

CANNIZZARO, J. P., AND K. L. CARDER. 2006. Estimating chlorophyll *a* concentrations from remote-sensing reflectance in optically shallow waters. Remote Sens. Environ. **101:** 13–24.

CAO, H-S., F.-X. KONG, L.-C. LUO, AND X.-L. SHI. 2006. Effects of wind and wind-induced waves on vertical phytoplankton distribution and surface blooms of *Microcystis aeruginosa* in Lake Taihu. J. Freshw. Ecol. **21:** 231–238.

CODD, G. A., S. G. BELL, K. KAYA, C. J. WARD, K. A. BEATTIE, AND J. S. METCALF. 1999. Cyanobacterial toxins, exposure routes and human health. Eur. J. Phycol. **34:** 405–415.

———, L. F. MORRISON, AND J. S. METCALF. 2005. Cyanobacterial toxins: Risk management for health protection. Toxicol. Appl. Pharmacol. **203:** 264–272.

DALL'OLMO, G., A. A. GITELSON, D. C. RUNDQUIST, B. LEAVITT, T. BARROW, AND J. HOLZ. 2005. Assessing the potential of SeaWiFS and MODIS for estimating chlorophyll concentration in turbid productive waters using red and near-infrared bands. Remote Sens. Environ. **96:** 176–187.

DEKKER, A. G. 1993. Detection of optical water quality parameters for eutrophic waters by high resolution remote sensing. Ph.D. thesis. Vrije Univ.

DOKULIL, M. T., AND K. TEUBNER. 2000. Cyanobacterial dominance in lakes. Hydrobiologia **438:** 1–12.

GEORGE, D. G., AND R. W. EDWARDS. 1976. The effect of wind on the distribution of chlorophyll a and crustacean plankton in a shallow eutrophic reservoir. J. Appl. Ecol. **13:** 667–690.

HADJIMITSIS, D. G., C. R. I. CLAYTON, AND V. S. HOPE. 2004. An assessment of the effectiveness of atmospheric correction algorithms through the remote sensing of some reservoirs. Int. J. Remote Sens. **25:** 3651–3674.

HAN, L., AND D. C. RUNDQUIST. 1997. Comparison of NIR/red ratio and first derivative of reflectance in estimating algal-chlorophyll concentration: A case-study in a turbid reservoir. Remote Sens. Environ. **62:** 253–261.

HAVENS, K. E., R. T. JAMES, T. L. EAST, AND V. H. SMITH. 2003. N : P ratios, light limitation, and cyanobacterial dominance in a subtropical lake impacted by non-point source nutrient pollution. Environ. Pollut. **122:** 379–390.

HEDGER, R. D., N. R. B. OLSEN, D. G. GEORGE, T. J. MALTHUS, AND P. M. ATKINSON. 2002. Coupling remote sensing with computational fluid dynamics modelling to estimate lake chlorophyll-*a* concentration. Remote Sens. Environ. **79:** 116–122.

———, N. R. B. OLSEN, D. G. GEORGE, T. J. MALTHUS, AND P. M. ATKINSON. 2004. Modelling spatial distributions of *Ceratium hirundnella* and *Microcystis* spp. in a small productive British lake. Hydrobiologia **528:** 217–227.

HUMPHRIES, S. E., AND V. D. LYNE. 1988. Cyanophyte blooms: The role of cell buoyancy. Limnol. Oceanogr. **33:** 79–91.

HUNTER, P. D., A. N. TYLER, M. PRÉSING, A. W. KOVÁCS, AND T. PRESTON. 2008. Spectral discrimination of phytoplankton colour groups: The effect of suspended particulate matter and sensor spectral resolution. Remote Sens. Environ. **112:** 1527–1544.

HYENSTRAND, P., P. BLOMQVIST, AND A. PETTERSSON. 1998. Factors determining cyanobacterial success in aquatic systems—a literature review. Arch. Hydrobiol. **51:** 41–62.

KROMKAMP, J., A. KONOPKA, AND L. R. MUR. 1988. Buoyancy regulation in light limited continuous cultures of *Microcystis aeruginosa*. J. Plankton Res. **10:** 171–183.

KUTSER, T. 2004. Quantitative detection of chlorophyll in cyanobacterial blooms by satellite remote sensing. Limnol. Oceanogr. **49:** 2179–2189.

———, L. METSAMAA, N. STRÖMBECK, AND E. VAHTMÄE. 2006. Monitoring phytoplankton blooms by satellite remote sensing. Estuar. Coast. Shelf Sci. **67:** 303–312.

LINDHOLM, T. J., J. E. ERIKSSON, AND J. A. O. MERILUOTO. 1989. Toxic cyanobacteria and water quality problems. Examples from a shallow eutrophic lake on Aland, South West Finland. Water Res. **23:** 481–486.

LORENZEN, C. J., AND S. W. JEFFREY. 1980. Determination of chlorophyll in seawater: Report of the intercalibration tests. UNESCO Technical Papers in Marine Science 35.

MADGWICK, F. J. 1999. Restoring nutrient-enriched shallow lakes: Integration of theory and practice in the Norfolk Broads, UK. Hydrobiologia **408:** 1–12.

MANTOURA, R. F. C., AND C. A. LLEWELLYN. 1983. The rapid-determination of algal chlorophyll and carotenoid pigments and their breakdown products in natural-waters by reverse-phase high performance liquid-chromatography. Anal. Chim. Acta **151:** 297–314.

MCQUEEN, D. J., AND D. R. S. LEAN. 1987. Influence of water temperature and nitrogen to phosphorus ratios on the dominance of blue-green algae in Lake St. George, Ontario. Can. J. Fish. Aquat. Sci. **44:** 598–604.

METSAMAA, L., T. KUTSER, AND N. STROMBECK. 2006. Recognising cyanobacterial blooms based on their optical signature: A modelling study. Boreal Environ. Res. **11:** 493–506.

OLIVER, R. L. 1994. Floating and sinking in gas-vacuolate cyanobacteria. J. Phycol. **30:** 161–173.

———, AND A. E. WALSBY. 1984. Direct evidence for the role of light-mediated gas vesicle collapse in the buoyancy regulation of *Anabaena flos-aquae* (cyanobacteria). Limnol. Oceanogr. **29:** 879–886.

PAERL, H. W. 1988. Nuisance phytoplankton blooms in coastal, estuarine and inland waters. Limnol. Oceanogr. **33:** 823–847.

PHILLIPS, G. L., A. KELLY, J. A. PITT, R. SANDERSON, AND E. TAYLOR. 2005. The recovery of a very shallow eutrophic lake, 20 years after the control of effluent derived phosphorus. Freshw. Biol. **50:** 1628–1638.

———, AND P. KERRISON. 1991. The restoration of the Norfolk Broads: The role of biomanipulation. Mem. Inst. Ital. Idrobiol. **48:** 75–97.

RANTAJÄRVI, E., R. OLSONEN, S. HÄLLFORS, J. M. LEPPÄNEN, AND M. RAATEOJA. 1998. Effect of sampling frequency on detection of natural variability in phytoplankton: Unattended high-frequency measurements on board ferries in the Baltic Sea. ICES J. Mar. Sci. **55:** 697–704.

REINART, A., AND T. KUTSER. 2006. Comparison of different satellite sensors in detecting cyanobacterial bloom events in the Baltic Sea. Remote Sens. Environ. **102:** 74–85.

REYNOLDS, C. S. 1973. Growth and buoyancy of *Microcystis aeruginosa* Kütz. emend. Elenkin in a shallow eutrophic lake. Proc. R. Soc. Lond. B **184:** 29–50.

———. 2006. Ecology of phytoplankton. Cambridge Univ. Press.

———, V. HUSZAR, C. KRUK, L. NASELLI-FLORES, AND S. MELO. 2002. Towards a functional classification of the freshwater phytoplankton. J. Plankton Res. **24:** 417–428.

———, R. L. OLIVER, AND A. E. WALSBY. 1987. Cyanobacterial dominance: The role of buoyancy regulation in dynamic lake environments. N. Z. J. Mar. Freshw. Res. **21:** 379–390.

———, AND D. A. ROGERS. 1976. Seasonal variations in the vertical distribution and buoyancy of *Microcystis aeruginosa* Kütz. Emend. Elenkin in Rostherne Mere, England. Hydrobiologia **48:** 17–23.

———, AND A. E. WALSBY. 1975. Water blooms. Biol. Rev. **50:** 437–481.

SARADA, R., M. G. PILLAI, AND G. A. RAVISHANKER. 1999. Phycocyanin from *Spirulina* sp: Influence of processing of biomass on phycocyanin yield, analysis of efficacy of extraction methods and stability studies on phycocyanin. Process Biochem **34:** 795–801.

SCHALLES, J. F., AND Y. Z. YACOBI. 2000. Remote detection and seasonal patterns of phycocyanin, carotenoid and chlorophyll pigments in eutrophic waters. Arch. Hydrobiol. Spec. Issues Adv. Limnol. **55:** 153–168.

SCHEFFER, M., S. RINALDI, A. GRAGNANI, L. R. MUR, AND E. H. VAN NES. 1997. On the dominance of filamentous cyanobacteria in shallow, turbid lakes. Ecology **78:** 272–282.

SIMIS, S. G. H., S. W. M. PETERS, AND H. J. GONS. 2005. Remote sensing of the cyanobacteria pigment phycocyanin in turbid inland water. Limnol. Oceanogr. **50:** 237–245.

———, A. RUIZ-VERDÚ, J. A. DOMiNGUEZ-GÓMEZ, R. PEÑA-MARTINEZ, S. W. M. PETERS, AND H. J. GONS. 2007. Influence of phytoplankton pigment composition on remote sensing of cyanobacterial biomass. Remote Sens. Environ. **106:** 414–427.

TAKAMURA, N., AND M. YASUNO. 1984. Diurnal changes in the vertical distribution of phytoplankton in hypertrophic Lake Kasumigaura, Japan. Hydrobiologia **112:** 53–60.

TYLER, A. N., E. SVÁB, T. PRESTON, M. PRÉSING, AND A. KOVACS. 2006. Remote sensing of the water quality of shallow lakes: A mixture modelling approach to quantifying phytoplankton in water characterised by high suspended sediment. Int. J. Remote Sens. **27:** 1521–1537.

VAN RIJN, J., AND M. SHILO. 1985. Carbohydrate fluctuations, gas vacuolation, and vertical migration of scum-forming cyanobacteria in fishponds. Limnol. Oceanogr. **30:** 1219–1228.

VILLAREAL, T. A., AND E. J. CARPENTER. 1990. Diel buoyancy regulation in the marine diazotrophic cyanobacterium *Trichodesmium thiebautii*. Limnol. Oceanogr. **35:** 1832–1837.

VINCENT, R. K., X. QIN, R. M. L. MCKAY, AND J. MINER. 2004. Phycocyanin detection from LANDSAT TM data for mapping cyanobacterial blooms in Lake Erie. Remote Sens. Environ. **89:** 381–392.

VISSER, P. M., H. A. M. KETELAARS, L. W. C. A. VAN BREEMEN, AND L. R. MUR. 1996. Diurnal buoyancy changes of *Microcystis* in an artificially mixed storage reservoir. Hydrobiologia **331:** 131–141.

WEBSTER, I. T. 1990. Effect of wind on the distribution of phytoplankton cells in lakes. Limnol. Oceanogr. **35:** 989–1001.

WORLD HEALTH ORGANIZATION [WHO]. 2003. Algae and cyanobacteria in fresh water, p. 136–158. *In* Guidelines for safe recreational water environments. Coastal and freshwaters. v. 1. World Health Organization.

WRIGHT, S. W., S. W. JEFFREY, R. F. C. MANTOURA, C. A. LLEWELLYN, T. BJØRNLAND, D. REPETA, AND N. WELSCH-MEYER. 1991. Improved HPLC method for the analysis of chlorophylls and carotenoids from marine phytoplankton. Mar. Ecol. Prog. Ser. **77:** 183–196.

ZOHARY, T., AND C. M. BREEN. 1989. Environmental factors favouring the formation of *Microcystis aeruginosa* hyper-scums in a hypertrophic lake. Hydrobiologia **178:** 179–192.